



# Numerical Study of Laterally Loaded Pile in Unsaturated Soils

L. M. Lalicata<sup>1</sup>(✉), G. M. Rotisciani<sup>1</sup>, A. Desideri<sup>1</sup>, F. Casini<sup>2</sup>,  
and L. Thorel<sup>3</sup>

<sup>1</sup> Department of Structural and Geotechnical Engineering (DISG),  
“Sapienza” University of Rome, Via Eudossiana 18, 00184 Rome, Italy  
leonardo.lalicata@uniroma1.it

<sup>2</sup> Department of Civil and Informatics Engineering (DICII),  
University of Rome “Tor Vergata”, Via Politecnico 1, 00133 Rome, Italy

<sup>3</sup> Institut Français Des Sciences et Technologies Des Transports,  
de L’aménagement et Des Réseaux (IFSTTAR), GERS Department,  
Geomaterials and Modelling in Geotechnics Laboratory, Bouguenais, France

**Abstract.** This note presents the preliminary outcomes of a numerical investigation on the influence of soil partial saturation on the behaviour of laterally loaded piles. The modified Cam clay model extended to unsaturated conditions and formulated in terms of Bishop’s effective stress has been used to analyse the results of centrifuge tests designed to address this topic. The model, calibrated on laboratory tests, well reproduces the main aspects of the soil-pile interaction. Load-deflection relationships and bending moments are analysed together with soil reactions against the pile and the strength mobilization level in the soil. The paper points out the significant changes in the pile response given by any variations in soil saturation conditions.

**Keywords:** Partial saturation · Constitutive modelling · Soil-structure interaction · Piles · Horizontal load · Bending moments

## 1 Introduction

Under lateral loadings, the kinematics of pile foundations typically involves a significant soil volume close to the surface. Studies based on the continuum approach with elastic or elasto-plastic models have shown that the response of flexible piles is largely influenced by relative pile-soil stiffness ratio, whereas for short and rigid piles, the response is affected by both stiffness and slenderness ratio (Budhu and Davies 1987; Randolph 1981; Di Laora and Rovithis 2015). Moreover, the non-linear soil behaviour strongly influences the main design parameters of the pile (head displacements, maximum bending moment, and critical length). In many applications, the significant soil volume is located above the water table and is frequently in partial saturation conditions. Lalicata *et al.* (2018) carried out a number of centrifuge tests devoted to investigate the effects of the variations in saturation level on the behaviour of laterally loaded pile. These tests have been numerically simulated using the modified Cam Clay Model extended to unsaturated conditions (Tamagnini 2004) for reproducing the

mechanical behaviour of soil. This work aims to: (i) validate the model for this class of boundary value problems; (ii) offer an insight into the processes taking place during the static loading and the rising of the water table. In the present note, after a brief description of the centrifuge tests, the numerical model is described together with the employed constitutive laws and the calibration procedure. Finally, the comparison between experimental data and numerical simulations is presented focusing on both pile and soil responses during the main phases of the tests.

## 2 Centrifuge Tests

Lalicata *et al.* (2018) conducted an experimental study on a small-scale laterally loaded pile installed in a commercial soil compacted on the dry side of the optimum Proctor curve (optimum water content  $w_{opt}$  and void ratio  $e_{opt}$  equal to 21% and 0.74, respectively). The authors performed 4 tests at  $100 \times g$  on a cylindrical model 180 mm high and 300 mm wide made of silty soil named B-grade kaolin (90% fine silt and 10% clay). The bored pile is installed at  $1 \times g$  in the centre of the model, the pre-hole is realized by a manual screwing system. The soil is statically compacted under oedometric conditions in six successive sub-layers, each approximately 30 mm thick.

In order to explore the influence of soil density, the models are prepared at two different void ratios (0.93 and 0.75) with the same water content  $w$  of 15.0%. A sand layer 1 cm thick is located at the bottom of the strongbox and is surrounded by geotextile. The model pile is a close-ended aluminium tube with a Young modulus  $E_p$  of 74 GPa, an external diameter  $D$  of 12 mm and internal diameter  $d$  equal to 10 mm, embedded for 150 mm in the soil. For each density, two water table levels,  $z_w$ , are considered:  $z_w = 0$  (saturated condition) and  $z_w = 70$  mm (unsaturated condition).

The experimental set up is depicted in Fig. 1. The soil vertical displacements are recorded by five LVDTs while the pore water pressures are measured via three tensiometers placed at different depths at the model border. One LVDT built in on a rotational joint gives pile's vertical displacement and rotation. Both lateral displacement and force at the load application point are given by a load cell, the bending moments along the pile are provided by 10 couples of strain gauges equally spaced every 15 mm.

After the pile installation, a zero pore pressure is applied at the model bottom in order to reduce after compaction suction (*Phase 1*). Then the strong-box is placed in the centrifuge, and the gravitational acceleration is quickly increased up to  $100 \times g$  (*Phase 2*) keeping the water table is at the desired level. Once stationary conditions are reached, the pile is loaded horizontally until the attainment of failure conditions in saturated soils and until a load of 1.2 MN and 2.1 MN in loose ( $e_0 = 0.93$ ) and dense ( $e_0 = 0.75$ ) unsaturated soils, respectively (*Phase 3*). Finally, in the last tests the water table is raised up to the mud line keeping constant the load (*Phase 4*).

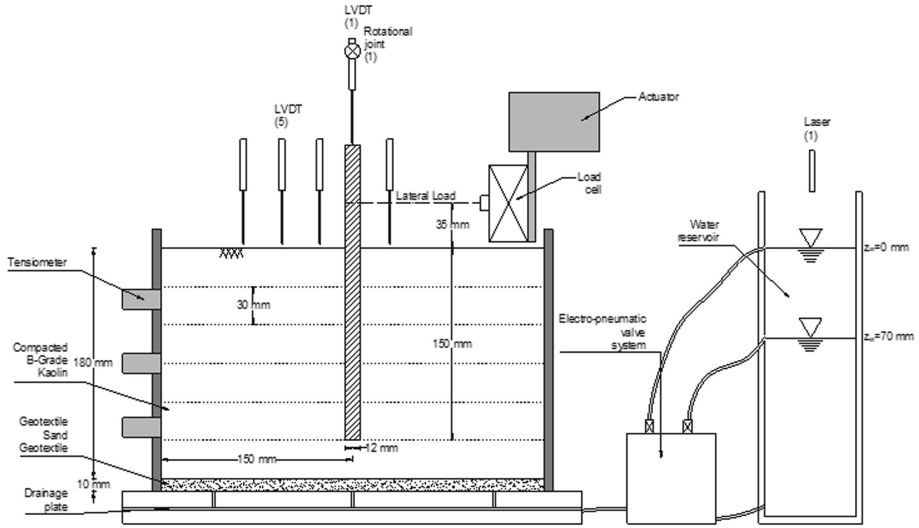


**Fig. 1.** Experimental set up and instrumentation, cross sectional view in the load plane (adapted from Lalicata *et al.* 2018).

### 3 Finite Element Model

#### 3.1 Hydro-Mechanical Model

The mechanical behaviour of the B-grade kaolin is described using the Modified Cam Clay Model extended to unsaturated conditions (Tamagnini 2004). This model is formulated in terms of Bishop's effective stresses. The mathematical formulation of this elastic-hardening plastic model is described in detail in Rotisciani *et al.* (2015). Here, only the main characteristics are reported.

Inside the yield surface, the model predicts an isotropic hypoelastic response characterized by a constant Poisson's ratio  $\nu$  and stiffness moduli varying with mean effective stress  $p'$  and specific volume and  $\nu$  and. The flow rule is assumed to be associated and the evolution of the yield surface is given by:

$$\dot{p}'_c = \frac{\nu p'_c}{\lambda - \kappa} \dot{\epsilon}'_v - b p'_c \dot{S}_r \quad (1)$$

where  $\lambda$  and  $\kappa$  are the slopes of the Normal Consolidation Line and the unloading-reloading line in a semi-logarithmic picture of the compressibility plane;  $b$  controls the evolution of the yielding surface with the variation of  $S_r$ . Thanks to the introduction of this additional term, the model is well-suited for describing the mechanical effects due to any variations of  $S_r$  (i.e. collapse upon wetting, changes in the preconsolidation stress).

The Water Retention Curve (WRC) is described by the well-known Van Genuchten expression:

$$S_r = S_{r,res} + (1 - S_{r,res})/[1 + (\alpha s)^n]^{1/(1-n)} \tag{2}$$

where  $S_{r,res}$  is the residual saturation degree and the parameters  $\alpha$  and  $n$  control the shape of the curve. The experimental data point out a marked influence of porosity on the retention behaviour; therefore, different WRCs have been adopted according to the

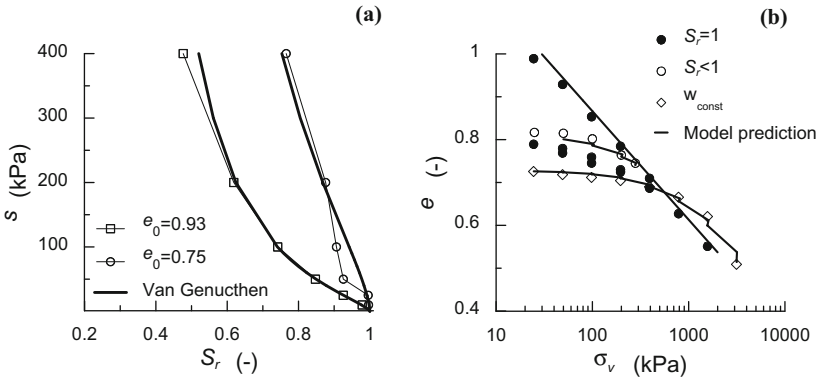


**Fig. 2.** (a) Water retention curve; (b) Oedometric tests.

initial void ratio (see Fig. 2a). The unsaturated permeability evolves with saturation degree according to the power law:  $k = k_{sat} S_r^3$ , where  $k_{sat}$  is saturated permeability ranging from 1.5 to 4.5  $10^{-9}$  m/s, depending on void ratio.

The constitutive laws have been calibrated against the results of oedometric tests carried out on a saturated soil sample and under suction controlled conditions. The predictive capabilities of the Modified Cam Clay model have been successively evaluated by numerically simulating an oedometric test performed at constant water content ( $w = 15\%$ ). As shown in Fig. 2b, the model well-reproduces the material response experimentally observed. The values for the constitutive parameters are listed in Table 1: the hydraulic parameters refer to soil samples prepared at the same void ratio as the model tested in centrifuge.

**Table 1.** Constitutive parameters.

Mechanical parameters						Hydraulic parameters			
v	$\kappa$	$\lambda$	M	$N_0$	b	$S_{r,res}$	$\alpha$	n	$k_{sat}$ (m/s)
0.25	0.04	0.11	0.86	1.36	3.7	0.16	0.02	1.4	$4.5 \cdot 10^{-9}$

### 3.2 Geometry and Boundary Conditions

Soil deformation mechanism varies depending on the phase of the centrifuge test considered, indeed:

1. Imbibition at  $1 \times g$  and in-flight phases occur under axial-symmetric conditions that reduce to one-dimensional deformation condition neglecting the presence of the pile;
2. Pile loading and subsequent water table rising at constant load take place in three-dimensional conditions.

Starting from these assumptions, two different geometrical models are carried out using the commercial code ABAQUS/standard. The first one is a simple 1D soil column model, while the second is a more sophisticated 3D model (Fig. 3a).

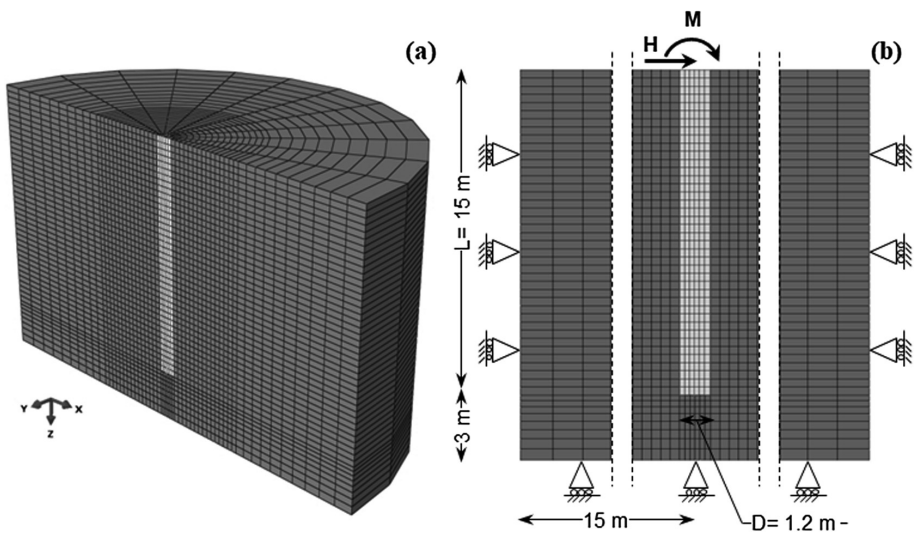


Fig. 3. (a) 3D model; (b) Symmetry plane.

The 1D model allows to fairly simulate the imbibition phase at  $1 \times g$  (*phase 1*), the increment of the total stress due to flight (*phase 2.1*) and the equalization process due to the application of the hydraulic boundary condition at the bottom (*phase 2.2*). The analysis outputs, such as effective stress, pore pressure and state variables distributions with depth, have been assumed as initial conditions of the 3D model which faithfully reproduces the geometry of the problem at the prototype scale (*phase 3*). For sake of brevity, the results of the 1D analysis will not be presented in this note.

The 3D model takes advantage of the symmetry along the vertical plane containing the force, allowing to model only half of the problem, Fig. 3b. The pile (embedded length  $L = 15 \text{ m}$ , diameter  $D = 1.2 \text{ m}$ ) is ideally installed in the centre of the soil layer  $18 \text{ m}$  thick and  $30 \text{ m}$  wide, after the initial geostatic step. Both Soil and pile are modelled as three-dimensional solid continuum porous elements. Beam elements with null stiffness (Young Modulus  $E = 1 \text{ kPa}$ ) are tied to the central nodes of the pile, in order to efficiently

obtain the bending moment profile along the pile length. Nodal displacements are fixed in the X, Y and Z directions at the base of the finite element mesh. The displacements at the lateral boundaries are constrained in the normal directions. The water table position and its variation are simulated by imposing the desired pore pressure value at the bottom of the model. In all the tests, the measured maximum bending moment lied well below the yielding value of 22 MNm. The pile is hence assumed to behave as a linear elastic material, whose stiffness (38.3 GPa) has been chosen in order to guarantee the same flexural rigidity ( $EI = 3.9 \text{ GNm}^2$ ) of the prototype tested (Lalicata *et al.* 2018), a value of 0.2 was assigned to Poisson's ratio. A purely frictional law is assigned at the soil-pile interface, a value of  $\delta = \varphi'/2$  is adopted both for shaft and base interfaces.

The load is applied at a master node to which the nodes of the pile's head are rigidly linked to move with. At the same node, a concentrated moment is applied to take into account the eccentricity of load in respect to ground level. The loading stage is modelled as a drained process according to the very low displacement rate imposed in the centrifuge test ( $v = 0.003 \text{ mm/min}$ ). After pile loading, the water table has been quickly raised up to the ground level increasing the pore pressure value at the model base. Then the transient consolidation is simulated until stationary or failure conditions are reached, whichever came first.

## 4 Results and Discussion

In this section, only the main aspects of the soil-pile interaction are presented focusing on the soil response during the loading process and water table rising. The comparison between experimental data and numerical predictions is presented for the two tests carried out on the soft soil ( $e_0 = 0.93$ ): in the first test the water table is at the ground level while in the second one is 7 m below it. According to the findings of the 1D analyses, the soil is assumed to be normally consolidated for both analyses.

### 4.1 Static Load

Figure 4a depicts the centrifuge data (CE) at the prototype scale in terms of load–deflection curves ( $H$ – $y$ ), where  $y$  represents the lateral deflection at the ground level. In the figure, diamonds and circles refer to the cases of  $z_w = 0$  and  $z_w = 7 \text{ m}$  respectively, while triangles describe the effects of the water table rising under a constant load ( $H = 1.2 \text{ MN}$ ). Numerical results (FEM), indicated by dashed and continuous lines, match quite well with experimental data. For the simulation of unsaturated soil condition two analyses have been performed: the first one, in black, follows the centrifuge test stages (loading and water table rising at constant load), while in the second (grey line) the load has been increased until soil failure.

In the range of lateral displacement explored, the load-displacement relationship is highly non-linear for the test in saturated soil (Mayne *et al.* 1995; Russo 2016). Under unsaturated conditions, the non-linearity of the response is less evident consistent with the well-known increment of preconsolidation stress in unsaturated soils (Gens 2010). The partial saturation induces higher stiffness and strength to the soil above the water table that strongly affects the pile response. Load-displacement relationship can be

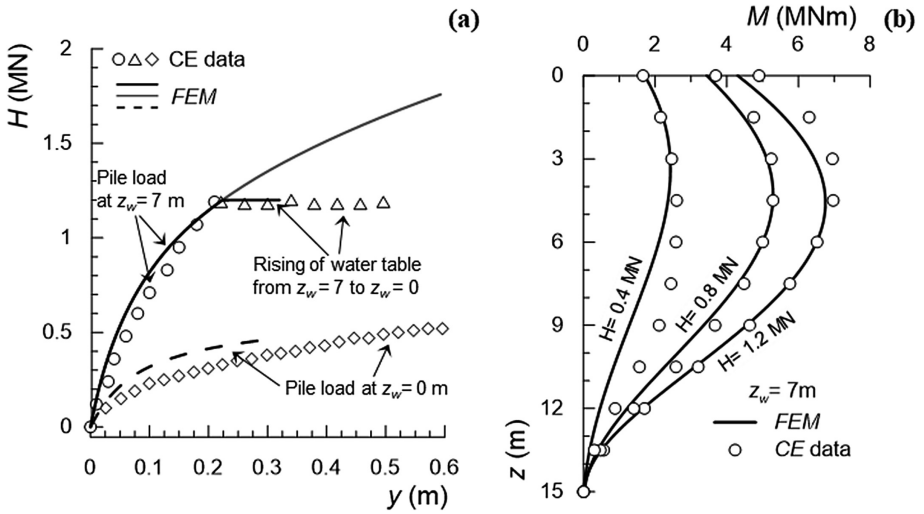


**Fig. 4.** (a) Load deflection relationship for tests in saturated ( $z_w = 0$ ) and unsaturated soil ( $z_w = 7$  m), comparison with numerical prediction; (b) Centrifuge data and model prediction of bending moment for  $z_w = 7$  m.

adequately fitted by means of a hyperbolic function (Mayne *et al.* 1995; Lalicata *et al.* 2018). This form is particularly useful as the fitting parameters have a clear physical meaning (ultimate load  $H_{lim}$  and the initial tangent  $K$ ). The best fitting procedure gives an ultimate load of 0.60 MN for saturated soil and 2.32 MN for unsaturated soil. Pile failure is conventionally attained when lateral deflection is about 10% of the diameter (0.12 m). At this displacement value the  $H/H_{lim}$  ratio predicted by the model is 0.4 for unsaturated soil test and 0.6 for the saturated soil condition, giving a reduction of mobilized load ratio of 33% in unsaturated soil condition compared to the saturated one. On the other hand, for low load levels, for example 0.2 MN, the head displacement is more than 3 times smaller in unsaturated soil condition. These considerations suggest that neglecting the effects of soil partial saturation leads to a significant underestimation of pile capacity. This underestimation can be reduced accounting properly the real soil behaviour.

The comparison between data and model predictions in terms of bending moment profiles ( $M$ ) at different load levels (0.4, 0.8 and 1.2 MN), are presented in Fig. 4b. The data refer to the test carried out on unsaturated soil. Globally, the model is capable of reproducing the experimental data, even though the match become more satisfying as the external load increases. Those differences are likely due to the installation effects neglected in the numerical model where the pile is ideally installed.

Figure 5 reports the profiles of deflection ( $y$ ), bending moment ( $M$ ) and soil reactions ( $P$ ) along the pile length for the two cases, at  $H = 0.28$  MN. The effect of the stiffness increase due to partial saturation stands out in the deflected shape and in the bending moment profile. Under saturated conditions, the rigid rotation (around a point 11.5 m deep) dominates the lateral deflection. On the other hand, under unsaturated conditions, the deflected shape tends to a flexible response and the displacement values are definitely

smaller compared to those obtained under saturated conditions. Bending moment profiles are consistent with the  $y$ -profiles: for  $z_w = 0$  m, significant values of moment are all along pile length (typical of rigid pile) while for  $z_w = 7$  m, below the maximum value, the moments tends to go sharply to zero (typical of flexible pile). The maximum value reduces of 33% as soil stiffness increases passing from saturated to unsaturated conditions and it moves upward passing from 6.0 m to 2.8 m from the pile head. Soil reactions against the pile are very different in the two cases. In particular, under unsaturated conditions, the maximum value of the reaction is attained near surface, and it gradually reduces moving downward. On the contrary, under saturated conditions, soil reaction starts from 0 at mud line and increases with depth as soil strength increases. The load used for this representation correspond to a loading ratio of about 0.46 and 0.12 for saturated and unsaturated soil condition respectively. Therefore the difference highlighted in Fig. 5 have to be ascribed on both the stiffness increase, related to the increase of mean effective stress, and the different levels of strength mobilization and plastic deformation developing in the soil for the various saturation condition.

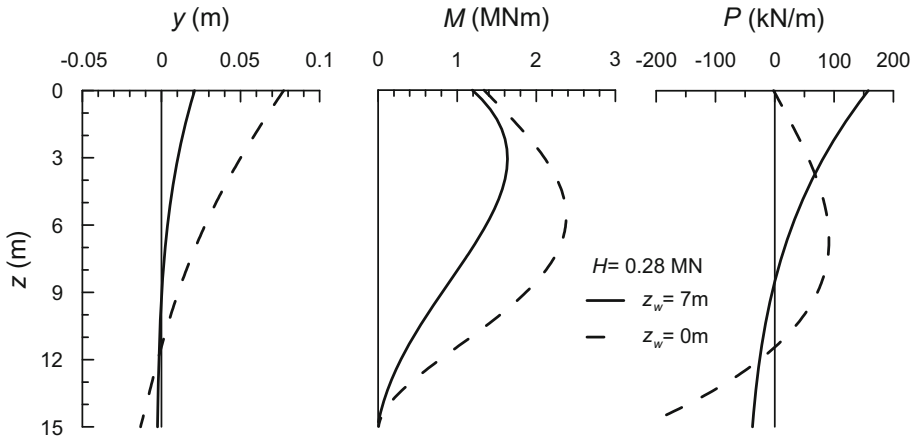


Fig. 5. Flexural response of the pile in function the elevation of the water table.

## 4.2 Water Table Rising

The loading stage in the analysis with water table 7 m below ground level ends at  $H = 1.2$  MN, then the water table rising and subsequent consolidation phase take place keeping unchanged the external load. Observing the temporal evolutions of the soil settlements and pore pressures, Lalicata *et al.* (2018) concluded that stationary conditions were not been reached at the end of the test, after 4 h of consolidation (centrifuge time). The reduction in strength related to the suction decrease during this stage led to the pile collapse with a rigid body motion: the pile head displacement greatly increased (Fig. 4a) with a small variation of maximum bending moment (less than 10%). The numerical model correctly captures these phenomena, even though the calculation ends early than the experimental data due to convergence difficulties.



The distortional strain contours depicted in Fig. 6 refer to the end of loading (Fig. 5a) and the last converged calculation of the consolidation process (Fig. 5b). Generally speaking, during static loading, the soil around the pile progressively fails starting from ground level (where there is the maximum interaction) and moving downward as the soil resistance is attained in the upper elements, Fig. 6. During the rising of the water table, distortional strains increase in magnitude and the soil volume involved in the interaction mechanism grows and deepens. Moreover, below the rotation point, on the left side, the rigid rotation of the pile entails a significant increase in the deviatoric strains.

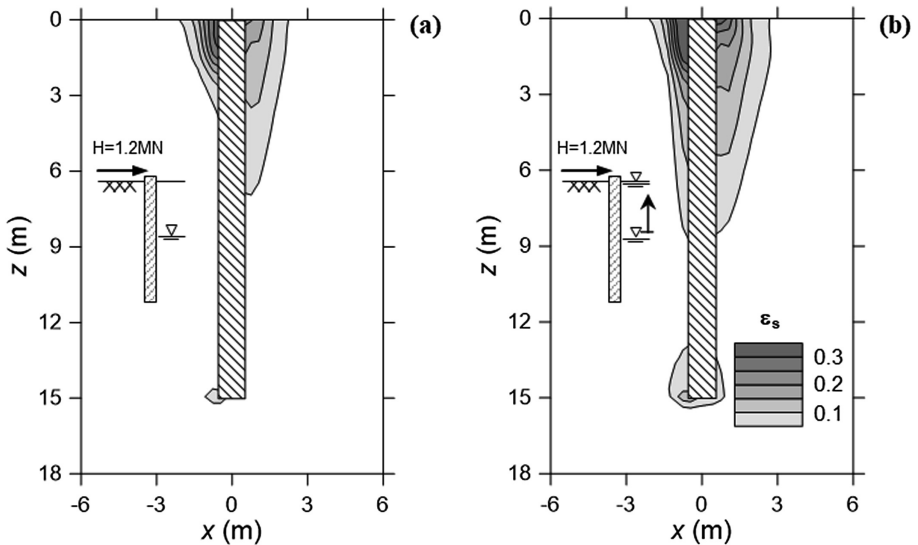


**Fig. 6.** Contour of distortional strain for  $z_w = 7$  m analysis: (a) Before the rising the water table; (b) After the rising of water table.

## 5 Conclusions

The study analyses the response of a single pile under static horizontal forces for two elevations of the water table, and, in unsaturated condition, its response to the water table rising. The soil stress-strain response has been modelled with the Modified Cam Clay Model extended to unsaturated conditions, the WRC is described by the Van Genuchten equation; both of them have been calibrated on the base of laboratory tests. The analyses have been performed with a three-dimensional model that correctly reproduces the geometry of the centrifuge tests conducted by Lalicata et al. (2018). A cost effective procedure has been implemented to define the soil condition prior to loading. The model predictions were found to be satisfactory compared with experimental results. Beyond the validation of the model, the simulations have allowed to clarify several aspects of the centrifuge tests such as the deflected shape of the pile and the

dependence of soil reactions from partial saturation. The analysis of the distortional strains in the soil during both static loading and water table rising has shown the deformation mechanism once reached failure conditions.

## References

- Budhu M, Davies TG (1987) Nonlinear analysis of laterally loaded piles in cohesionless soils. *Can Geotech J* 24(2):289–296
- Di Laora R, Rovithis E (2015) Kinematic bending of fixed-head piles in nonhomogeneous soil. *J Geotech Geoenvironmental Eng* 141(4):04014126. [https://doi.org/10.1061/\(ASCE\)GT.1943-5606.0001270](https://doi.org/10.1061/(ASCE)GT.1943-5606.0001270)
- Gens A (2010) Soil–environment interactions in geotechnical engineering. *Géotechnique* 60(1):3–64
- Krishnan R, Gazetas G, Velez A (1983) Static and dynamic lateral deflexion of piles in non – homogeneous soil stratum. *Géotechnique* 33(3):307–325
- Lalicata L, Desideri A, Casini F, Thorel L (2018) Experimental observation on a laterally loaded pile in unsaturated silty soil. *Can Geotech J*. <https://doi.org/10.1139/cgj-2018-0322>
- Mayne PW, Kulhawy FH, Trautmann CH (1995) Laboratory modeling of laterally-loaded drilled shafts in clay. *J Geotech Eng* 121(12):827–835
- Randolph MF (1981) The response of flexible piles to lateral loading. *Géotechnique* 31(2):247–259
- Rotisciani GM, Casini F, Desideri A, Sciarra G (2017) Hydromechanical behavior of an embankment during inundation. *Can Geotech J* 54:348–358
- Rotisciani GM, Sciarra G, Casini F, Desideri A (2015) Hydro-mechanical response of collapsible soils under different infiltration events. *Int J Numer Anal Meth Geomech* 39(11):1212–1234. <https://doi.org/10.1002/nag.2359>
- Russo G (2016) A method to compute the non-linear behaviour of piles under horizontal loading. *Soils Found* 56(1):33–43
- Soranzo E, Tamagnini R, Wu W (2015) Face stability of shallow tunnels in partially saturated soil: centrifuge testing and numerical analysis. *Géotechnique* 65(6):454–467
- Tamagnini R (2004) An extended cam-clay model for unsaturated soils with hydraulic hysteresis. *Géotechnique* 54(3):223–228